

A SPARSE GRAPH FORMULATION FOR EFFICIENT SPECTRAL IMAGE SEGMENTATION

Rahul Palnitkar

Haverford College
Department of Computer Science
370 Lancaster Avenue
Haverford, PA 19041

Jeova Farias Sales Rocha Neto

Bowdoin College
Department of Computer Science
255 Maine Street
Brunswick, ME 04011

ABSTRACT

Spectral Clustering is one of the most traditional methods to solve segmentation problems. Based on Normalized Cuts, it aims at partitioning an image using an objective function defined by a graph. Despite their mathematical attractiveness, spectral approaches are traditionally neglected by the scientific community due to their practical issues and underperformance. In this paper, we adopt a sparse graph formulation based on the inclusion of extra nodes to a simple grid graph. While the grid encodes the pixel spatial disposition, the extra nodes account for the pixel color data. Applying the original Normalized Cuts algorithm to this graph leads to a simple and scalable method for spectral image segmentation, with an interpretable solution. Our experiments also demonstrate that our proposed methodology over performs both traditional and modern unsupervised algorithms for segmentation in both real and synthetic data.

Index Terms— Image Segmentation, Spectral Clustering, Sparse Matrices, Optimization.

1. INTRODUCTION

Image Segmentation refers to the problem of grouping image pixels in meaningful regions with the goal of understanding or summarizing the visual content in that image [1]. Because of that, image segmentation has found applications in many domains, such as medical image analysis, autonomous driving, and photo editing to name a few [1]. This intense industrial appeal led to the development of many algorithms, which tackled the problem using variational [2], graphical [3, 4], statistical [5] and, more recently, deep learning techniques [6].

Normalized Cuts (NCut) [3] provides one of the most classical algorithms for image segmentation, and it stands out for its methodological consistency backed by graph theory and computational linear algebra. It consists of encoding the image data into a graph then using spectral techniques to approximately find the cut corresponding to the final segmentation. Overall, it has been an enduring algorithm for vision problems [7], and is currently receiving prodigious research interest due to the emergence of Vision Transformers

[8], because of its capacity to automatically detect objects and segment images using Transformer-based image embeddings, such as those arising from DINO architectures [9] or other self-supervised methodologies [10].

Despite its persistent theoretical appeal, NCut’s initial formulation rapidly met with drawbacks that would hinder its broader adoption by the scientific community, although many strategies were approached to overcome them [7, 11, 12]. The issues mostly were (1) computational, as it required handling large matrices [7], and (2) practical, as it performed worse than other unsupervised segmentation algorithms [13].

In this paper, we address both issues by adopting a sparse graph consisting of a grid graph that encodes the pixel spatial locations and of a few extra nodes corresponding to the pixel intensities [2, 4]. We show that the NCut solution found using this graph is *interpretable*, as it encourages pixel groupings that linearly balance spatial coherence (neighbors generally belong to the same group) and color cohesion (pixels in a segment have colors in the same subset of colors) [14]. Furthermore, we also demonstrate that this simple spectral formulation is *scalable*, and that *its only parameter has a clear interpretation*, which eases its tuning. We compare our method to other traditional and modern unsupervised techniques for segmentation and observe that *it outperforms its spectral counterparts* in terms of runtime and quality, while also being competitive against the other methods.

2. BACKGROUND

2.1. Normalized Cuts

Let I be an image of n pixels and k unique colors. Let $G = (V, E, w)$ be an undirected weighted graph where each node corresponds to a pixel and the weight function $w(i, j)$ evaluates the similarity between pixels i and j . A binary segmentation of I is achieved by finding a partition (A, B) of V that minimizes the cut value $\text{Cut}(A, B) = \sum_{i \in A, j \in B} w(i, j)$.

This approach however favors unbalanced partitions, leading to undesirable solutions. A way of addressing this is

to consider the normalized cut value $\text{NCut}(A, B)$ [3] instead,

$$\text{NCut}(A, B) = \frac{\text{Cut}(A, B)}{\text{Vol}(A)} + \frac{\text{Cut}(A, B)}{\text{Vol}(B)},$$

where $\text{Vol}(A) = \sum_{i \in A, j \in V} w(i, j)$ is a measure of the ‘‘volume’’ of A . We use $\text{Vol}(V) = \text{Vol}(A) + \text{Vol}(B)$ to represent the volume of all edges in G .

Let W be the weighted adjacency matrix of G and D be the diagonal degree matrix with $D(i, i) = \sum_{j \in V} w(i, j)$. The Laplacian matrix of G is then defined as $L = D - W$. Following the derivation presented in [15], we can write the problem of minimizing the NCut of G as:

$$\begin{aligned} \min_{\mathbf{x}} \quad & \mathcal{E}(\mathbf{x}|G), \\ \text{s.t.} \quad & \mathbf{x}^\top D \mathbf{x} = 1, \quad \mathbf{1}^\top D \mathbf{x} = 0, \quad \mathbf{x} \in \{-\alpha, \beta\}^n. \end{aligned} \quad (1)$$

where \mathbf{x} is the vector that corresponds to our final segment assignment, $\mathcal{E}(\mathbf{x}|G) = \mathbf{x}^\top L \mathbf{x}$ is the objective function or *assignment energy* we wish to minimize and:

$$\alpha = \sqrt{\frac{\text{Vol}(A)}{\text{Vol}(V) \text{Vol}(B)}}, \quad \beta = \sqrt{\frac{\text{Vol}(B)}{\text{Vol}(V) \text{Vol}(A)}}. \quad (2)$$

The algorithm in [3], here called the NCut algorithm, solves a relaxation of the minimum NCut problem by dropping the integer constraint in Eq. 1. The new optimization problem can be solved via generalized eigenvector decomposition,

$$L \mathbf{x} = \lambda D \mathbf{x}. \quad (3)$$

The algorithm then selects the eigenvector \mathbf{x} with second-smallest eigenvalue, and partitions V by thresholding \mathbf{x} [3].

2.2. Classical Edge Weight for Image Segmentation

A crucial step in developing efficient segmentation solvers using NCut is to define how the function w is computed. In the original NCut work and in early subsequent work [16, 17], the w combined two grouping cues in a single value:

$$\begin{aligned} w(i, j) = \exp \left(-\frac{\|I(i) - I(j)\|^2}{2\sigma_I^2} - \frac{\|X(i) - X(j)\|^2}{2\sigma_X^2} \right) \\ \times \mathbb{1}(\|X(i) - X(j)\| < r), \end{aligned} \quad (4)$$

where $I(j)$ and $X(j)$ are the appearance (such as the color) of pixel j and its spatial location on image I , respectively, $\mathbb{1}(\cdot)$ is the indicator function, and r , σ_I and σ_X have fixed values.

2.3. Drawbacks of the Traditional Approach

The NCut formulation based on the above weight function presents several drawbacks. For one, it is computationally inefficient to construct the above graph for high resolution images, since it requires visiting each pixel and their neighboring locations within a radius r . Secondly, this graph is potentially dense, which poses memory and runtime issues during eigenvector computation. NCut with weights as in Eq. 4 is also known to be underperforming in practice [13].

Moreover, calibrating the values for σ_X and σ_I is challenging [14]. Finally, the optimization in Eq. 1 on the graph

constructed using Eq. 4 lacks interpretability [14]. The only understanding we can extract from its solution is that it encourages similar pixels to be grouped together, which is commonplace for any spectral clustering algorithm.

3. PROPOSED METHODOLOGY

3.1. New Graph Formulation

Inspired by [4] and [2], we show that a sparse graph formulation efficiently tackles the issues with the classical NCut formulation. Our graph construction starts by considering a grid graph G_{grid} whose vertices correspond to image pixels, with edges of weight $\mu > 0$ between each pair of neighboring pixels. From G_{grid} , we create a new graph G_{all} by adding k extra nodes, each corresponding to one of the k unique colors in I . Each node on G_{grid} is then connected to the extra node corresponding to its color with an edge of unitary weight. This graph formulation is computationally attractive for its sparsity. Assuming $k \ll n$, G_{all} only requires $O(n)$ edges. When segmenting I , we only make use of the assignment vector for the grid nodes.

3.2. Interpretation of the Cut on G_{all}

Let W_{grid} and L_{grid} be the adjacency and Laplacian matrices of G_{grid} , respectively. Let W_{all} and L_{all} be the analogous to G_{all} . These matrices are related to each other as follows:

$$W_{\text{all}} = \begin{bmatrix} W_{\text{grid}} & H \\ H^\top & 0 \end{bmatrix}, \quad L_{\text{all}} = \begin{bmatrix} L_{\text{grid}} + I & -H \\ -H^\top & D_n \end{bmatrix}$$

where $H \in \mathbb{R}^{n \times k}$ is a one-hot encoding of the colors in I , i.e. $H(i, j) = \mathbb{1}\{I(i) = j\}$, and $D_n \in \mathbb{R}^{k \times k}$ is diagonal such that $D_n(j, j) = n_j$, where n_j is the number of pixels in I with color j . Let \mathbf{x} and \mathbf{y} be the assignment vectors for the nodes in G_{grid} and for the extra nodes, respectively. Note that $\mathbf{x} \in \{-\alpha, \beta\}^n$ and $\mathbf{y} \in \{-\alpha, \beta\}^k$, where α and β are computed using Eq. 2 on the graph G_{all} . Let $\mathbf{z} = [\mathbf{x}|\mathbf{y}]$ be \mathbf{x} and \mathbf{y} concatenated. The objective in Eq. 1 then becomes:

$$\begin{aligned} \mathcal{E}(\mathbf{z}|G_{\text{all}}) &= \mathbf{z}^\top L_{\text{all}} \mathbf{z} \\ &= \mathbf{x}^\top (L_{\text{grid}} + I) \mathbf{x} - 2(H\mathbf{y})^\top \mathbf{x} + \mathbf{y}^\top D_n \mathbf{y}. \end{aligned} \quad (5)$$

Noticing that $D_n = H^\top H$, we derive the energy associated with the assignment \mathbf{z} of the nodes on G_{all} :

$$\mathcal{E}(\mathbf{z}|G_{\text{all}}) = \|\mathbf{x} - H\mathbf{y}\|_2^2 + \mathbf{x}^\top L_{\text{grid}} \mathbf{x}. \quad (6)$$

The first term in the above expression accounts for the number of pixels that are assigned to a partition that is not the same as the partition its color is assigned to. In fact, if we define n_{mismatch} as the number of these mismatches, we have:

$$\|\mathbf{x} - H\mathbf{y}\|_2^2 = (\alpha + \beta)^2 n_{\text{mismatch}}. \quad (7)$$

Because of the grid nature of G_{grid} , the second term in Eq. 6 accounts for the number of neighboring pixel pairs that are assigned to different segments:

$$\mathbf{x}^\top L_{\text{grid}} \mathbf{x} = \mu(\alpha + \beta)^2 n_{\text{boundary}}, \quad (8)$$

Fig. 1: Quantitative results on synthetic images in terms of mIoU and average runtime. The greater the mIoU value, the better.

Noise Type	Noise Param.												
		Ours	NCut	MixNCut	MGSC	Ours	NCut	MixNCut	MGSC	Ours	NCut	MixNCut	MGSC
Gauss.	$\sigma_g^2 = 0.5$	0.967	0.434	0.965	0.920	0.981	0.358	0.985	0.958	0.980	0.745	0.981	0.973
	$\sigma_g^2 = 1.5$	0.859	0.244	0.828	0.720	0.926	0.304	0.938	0.865	0.908	0.515	0.919	0.808
S&P	$d = 0.3$	0.964	0.570	0.906	0.903	0.992	0.531	0.959	0.931	0.981	0.788	0.945	0.983
	$d = 0.7$	0.927	0.383	0.685	0.889	0.975	0.330	0.725	0.830	0.952	0.598	0.825	0.950
Average Runtime (s)		0.27	13.41	14.30	167.64	0.21	12.92	15.48	147.45	0.19	12.89	13.08	157.81

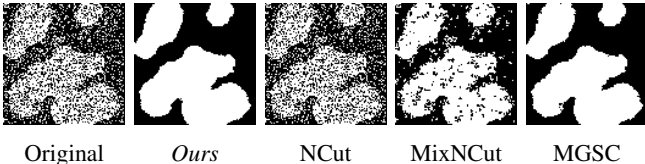


Fig. 2: Qualitative results on synthetic images. The original image is contaminated with Salt & Pepper noise, $d = 0.7$.

where n_{boundary} stands for the number of pixels on the boundary of the final segmentation. Finally, noticing that $(\alpha + \beta)^2 = \text{Vol}(V) / (\text{Vol}(A) \text{Vol}(B))$ from Eq. 2, we have that:

$$\mathcal{E}(z|G_{\text{all}}) = \frac{\text{Vol}(V)}{\text{Vol}(A) \text{Vol}(B)} (n_{\text{mismatch}} + \mu n_{\text{boundary}}). \quad (9)$$

Minimizing $\mathcal{E}(z|G_{\text{all}})$ for \mathbf{x} and \mathbf{y} , results in finding a partition of G_{all} that trades off between spacial coherence (neighboring pixels should belong to the same segment) and color cohesion (pixels in a segment should have colors belonging to the same subset of available intensities) via the value of μ . Minimizing the multiplicative factor in Eq. 9 also encourages a balanced partition of the nodes in G_{all} .

4. NUMERICAL EXPERIMENTS

4.1. Experimental Setup

We proceed with experiments on real and synthetic images. For our synthetic results, we contaminate three different background and foreground square patterns (intensities of either 0 and 1) of side length ℓ with either additive zero mean and variance σ_g^2 Gaussian noise or Salt & Pepper (S&P) with noise density d . The generated images are then rescaled and discretized, so the color intensities are integers in $[0, 255]$. We also test our method using all the 500 images of the BSDS500 dataset [13]. For each of them, we vectorize the RGB color space using mini-batch K -means clustering [18] with $k = 256$ as a preprocessing stage for our proposed method only.

Since the images in our real dataset may contain multiple objects/segments in their ground-truth, we generalized our proposed binary segmentation method taking the prescription in [3] as inspiration. Here, we recursively reapply our proposed method on the partitions found by it until the energy

$\mathcal{E}(z|G_{\text{all}})$ (ref. Eq. 5) of that partition is below given a threshold (set to 0.01) or until a given partition had already been subdivided 3 times.

For performance evaluation, we assess the segmentations via the intersection over union $\text{IoU} = |R \cap S| / |R \cup S|$, where R and S are a ground truth image region and its predicted segmentation, respectively. We then computed the mean IoU (mIoU) by averaging the IoU values over the image [19]. The predicted segments are matched one-to-one with target segments using a version of the Hungarian algorithm modified to accommodate when the number of segments in the final segmentation is different from that of the ground truth. BSDS provides multiple ground-truth segmentations, so we average their respective mIoU's to get our final measure.

We compare our proposed method with NCut and two more spectral methods for unsupervised segmentation, Multi Graph Spectral Clustering (MGSC) [20] and MixNCut [14] in our synthetic experiments. For our real data, we compare our results to those of three traditional baselines, K -means, Graph-based Segmentation (GS) [21] and SLIC [22]; and five state-of-the-art deep learning-base unsupervised segmentation algorithms, DFC [19], IIC [23], PiCIE [18], SegSort [24], and W-Net [25]. W-Net is of particular interest to us, as it using Normalized Cuts concepts to devise its segmentation technique. Parameter tuning and model selection is performed in each method. When using all these techniques, we refrain from any sparsification algorithm. For NCut, we also set $r = \infty$ in Eq. 4 so that we can compare similar graph formulations. In our synthetic experiments, we apply NCut on the full pixel set. In the experiments using BSDS500, we first use SLIC [22] to oversegment the image in 500 superpix-

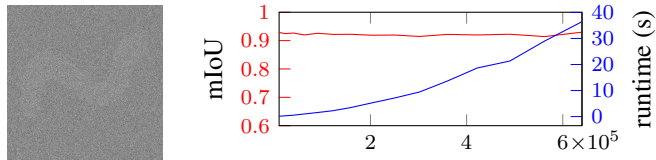


Fig. 3: Segmentation results for varying image sizes. Left: a sample image for $\ell = 500$. Right: performance results varying the number of image pixels $n = \ell^2$.

Table 1: Quantitative results on BSDS500 dataset. We set $\mu = 0.01$ in our method. †The value listed is sourced from [19].

Algorithm	NCut	SLIC	K -means†	GS†	IIC †	DFC†	DoubleDIP	PiCIE	W-Net	SegSort	Ours
mIoU	0.385	0.137	0.240	0.313	0.172	0.305	0.356	0.325	0.428	0.480	0.479

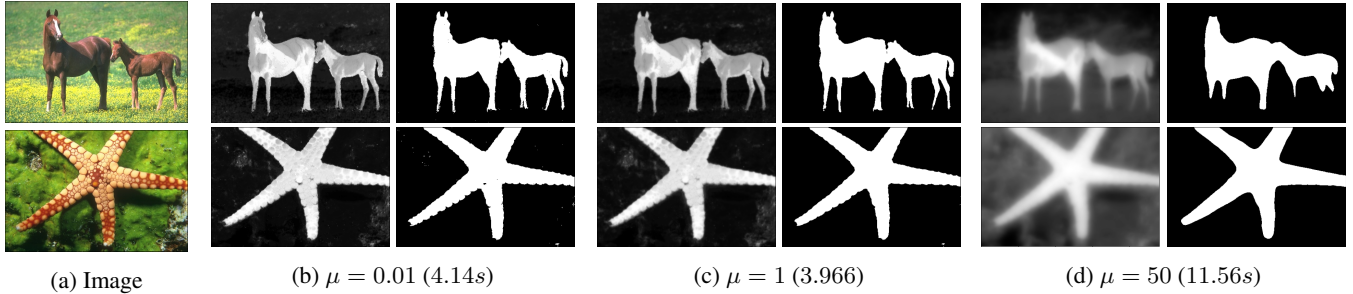


Fig. 4: Qualitative results on BSDS500 images for various μ . (b)-(d) show the eigenvector from Eq. 3 (left) and the corresponding segmentation (right). Both images are of size 481×321 and the average segmentation runtime is shown in parentheses.

els for memory savings. We also apply the recursive strategy above for NCut when segmenting multiregion images.

The experiments ran on an Apple M1 Pro Chip (8 core CPU, 14 core GPU) with 16 Gb of RAM memory and were coded in Python 3.9.7 using Numpy 1.21.4 and Scipy 1.7.3¹.

4.2. Results and Discussion

In Table ??, we show the quantitative assessment of our proposed method for images with $\ell = 100$ pixels and the two different noise contaminations when generating each synthetic image under the three proposed ground-truth patterns. For our method, we depict the best mIoU when considering $\mu \in [0, 1, \dots, 10]$. In the same table, we also display the average runtime for generating each of the best results’ performance in each method per pattern. In Figure 2, we qualitatively compare the best results of each method under a challenging Gaussian noise level. These results demonstrate that our method greatly over performs its related spectral methods in terms of runtime, a consequence of its sparse nature, while also being competitive in terms of mIoU, attaining almost perfect segmentations in most challenging scenarios.

In Figure 3, we present our average performance for images arising from the three patterns in Table ?. We vary ℓ and contaminate each image with Gaussian noise, $\sigma_g^2 = \ell/100$, i.e. the images become increasingly noisier with size. An example is shown in Figure 3. These results demonstrate that our method scales well despite its spectral nature and generates high quality segmentations on large images even in very challenging noise settings. The runtime growth depicted in Figure 3 also reflects our method’s linear complexity.

In Figure 4, we evaluate the effect of μ on binary segmentation of images and qualitatively demonstrate our method’s performance and runtime in two BSDS500 images. Here, we

note that μ has the effective role of “blurring” the eigenvector and, consequently, smoothing the borders of the final segmentation, removing artifacts or boundary details as it increases. Such a clear and straightforward parameter interpretation is not present in the traditional formulation of Eq. 4, which entails that tuning it for a specific need is also simpler.

In Table 1, we quantitatively demonstrate the mIoU performance of our proposed method on BSDS data, comparing it to other unsupervised segmentation algorithms. Firstly, note that NCut and W-Net, whose conceptual basis is also NCut, perform surprisingly well compared to the other baselines and outperforms many Deep Learning methods. This can be seen as evidence for the power of spectral formulations to unsupervised segmentation tasks. Secondly, we note that our method is only outperformed, slightly, by SegSort, which despite being unsupervised still makes use of pretrained deep learning features. This means that our simple methodology, which uses just color data, performs as well as other methods that rely on richer, but harder to train, features, demonstrating the suitability and appeal of our formulation to segmentation.

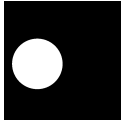
5. CONCLUSION

In this paper, we introduce a new spectral algorithm for image segmentation that overcomes some historical issues found in the NCut framework and in its related methods. We employ an efficient sparse graph, whose usage under the traditional NCut optimization problem leads to an interpretable cut value. We also show that our method, which is fully characterized by just one parameter, is fast and produces high quality results under high synthetic noise settings, and outperforms many state-of-the art unsupervised image segmentation algorithm on a popular RGB image dataset. These results demonstrate the effectiveness of using our sparse formulation for spectral image segmentation.

¹A demo code for this paper is available at www.github.com/raahul-palnitkar/Sparse-Graph-Spectral-Segmentation.

6. REFERENCES

- [1] Richard Szeliski, *Computer vision: algorithms and applications*, Springer Nature, 2022.
- [2] Leo Grady, “Multilabel random walker image segmentation using prior models,” in *Proceedings of the IEEE ICCV*. IEEE, 2005, vol. 1, pp. 763–770.
- [3] Jianbo Shi and Jitendra Malik, “Normalized cuts and image segmentation,” *IEEE TPAMI*, vol. 22, no. 8, pp. 888–905, 2000.
- [4] Meng Tang, Lena Gorelick, Olga Veksler, and Yuri Boykov, “Grabcut in one cut,” in *Proceedings of the IEEE ICCV*, 2013, pp. 1769–1776.
- [5] Jeova FS Rocha Neto, Pedro Felzenszwalb, and Marilyn Vazquez, “Direct estimation of appearance models for segmentation,” *SIAM Journal on Imaging Sciences*, vol. 15, no. 1, pp. 172–191, 2022.
- [6] Shervin Minaee, Yuri Y Boykov, Fatih Porikli, Antonio J Plaza, et al., “Image segmentation using deep learning: A survey,” *IEEE TPAMI*, 2021.
- [7] Charless Fowlkes, Serge Belongie, et al., “Spectral grouping using the nystrom method,” *IEEE TPAMI*, vol. 26, no. 2, pp. 214–225, 2004.
- [8] Kai Han, Yunhe Wang, Hanting Chen, Xinghao Chen, Jianyuan Guo, Zhenhua Liu, Yehui Tang, An Xiao, et al., “A survey on vision transformer,” *IEEE TPAMI*, vol. 45, no. 1, pp. 87–110, 2022.
- [9] Xudong Wang, Rohit Girdhar, Stella X Yu, and Ishan Misra, “Cut and learn for unsupervised object detection and instance segmentation,” in *Proceedings of the IEEE CVPR*, 2023, pp. 3124–3134.
- [10] Luke Melas-Kyriazi, Christian Rupprecht, Iro Laina, and Andrea Vedaldi, “Deep spectral methods: A surprisingly strong baseline for unsupervised semantic segmentation and localization,” in *Proceedings of the IEEE CVPR*, 2022, pp. 8364–8375.
- [11] Li He, Nilanjan Ray, Yisheng Guan, and Hong Zhang, “Fast large-scale spectral clustering via explicit feature mapping,” *IEEE transactions on cybernetics*, vol. 49, no. 3, pp. 1058–1071, 2018.
- [12] Lingfei Wu, Pin-Yu Chen, Ian En-Hsu Yen, Fangli Xu, Yinglong Xia, and Charu Aggarwal, “Scalable spectral clustering using random binning features,” in *Proceedings of the 24th ACM SIGKDD*, 2018, pp. 2506–2515.
- [13] Pablo Arbelaez, Michael Maire, Charless Fowlkes, and Jitendra Malik, “Contour detection and hierarchical image segmentation,” *IEEE TPAMI*, vol. 33, no. 5, pp. 898–916, 2010.
- [14] Jeova FS Rocha Neto and Pedro F Felzenszwalb, “Spectral image segmentation with global appearance modeling,” *arXiv e-prints*, pp. arXiv–2006, 2020.
- [15] Tijn De Bie and Nello Cristianini, “Fast sdp relaxations of graph cut clustering, transduction, and other combinatorial problems,” *The Journal of Machine Learning Research*, vol. 7, pp. 1409–1436, 2006.
- [16] Lihi Zelnik-Manor and Pietro Perona, “Self-tuning spectral clustering,” *NeuRIPS*, vol. 17, 2004.
- [17] Wenbing Tao, Hai Jin, and Yimin Zhang, “Color image segmentation based on mean shift and normalized cuts,” *IEEE Transactions on Cybernetics*, vol. 37, no. 5, pp. 1382–1389, 2007.
- [18] Jang Hyun Cho, Utkarsh Mall, Kavita Bala, and Bharath Hariharan, “Picie: Unsupervised semantic segmentation using invariance and equivariance in clustering,” in *Proceedings of the IEEE CVPR*, 2021, pp. 16794–16804.
- [19] Wonjik Kim, Asako Kanezaki, and Masayuki Tanaka, “Unsupervised learning of image segmentation based on differentiable feature clustering,” *IEEE Transactions on Image Processing*, vol. 29, pp. 8055–8068, 2020.
- [20] Dengyong Zhou and Christopher JC Burges, “Spectral clustering and transductive learning with multiple views,” in *Proceedings of the 24th ICML*, 2007, pp. 1159–1166.
- [21] Pedro F Felzenszwalb and Daniel P Huttenlocher, “Efficient graph-based image segmentation,” *International journal of computer vision*, vol. 59, pp. 167–181, 2004.
- [22] Radhakrishna Achanta, Appu Shaji, Kevin Smith, Aurelien Lucchi, Pascal Fua, and Sabine Süsstrunk, “Slic superpixels compared to state-of-the-art superpixel methods,” *IEEE TPAMI*, vol. 34, no. 11, pp. 2274–2282, 2012.
- [23] Xu Ji, Joao F Henriques, and Andrea Vedaldi, “Invariant information clustering for unsupervised image classification and segmentation,” in *Proceedings of the IEEE ICCV*, 2019, pp. 9865–9874.
- [24] Jyh-Jing Hwang, Stella X Yu, Jianbo Shi, Maxwell D Collins, Tien-Ju Yang, Xiao Zhang, and Liang-Chieh Chen, “Segsort: Segmentation by discriminative sorting of segments,” in *Proceedings of the IEEE ICCV*, 2019, pp. 7334–7344.
- [25] Xide Xia and Brian Kulis, “W-net: A deep model for fully unsupervised image segmentation,” *arXiv preprint arXiv:1711.08506*, 2017.

mIoU	Noise Type	Noise Param.												
			<i>Ours</i>	NCut	MixNCut	MGSC	<i>Ours</i>	NCut	MixNCut	MGSC	<i>Ours</i>	NCut	MixNCut	MGSC
Gauss.	$\sigma_g^2 = 0.5$		0.967	0.434	0.965	0.920	0.981	0.358	0.985	0.958	0.980	0.745	0.981	0.973
	$\sigma_g^2 = 1.5$		0.859	0.244	0.828	0.720	0.926	0.304	0.938	0.865	0.908	0.515	0.919	0.808
S&P	$d = 0.3$		0.964	0.570	0.906	0.903	0.992	0.531	0.959	0.931	0.981	0.788	0.945	0.983
	$d = 0.7$		0.927	0.383	0.685	0.889	0.975	0.330	0.725	0.830	0.952	0.598	0.825	0.950
Average Runtime (s)			0.27	13.41	14.30	167.64	0.21	12.92	15.48	147.45	0.19	12.89	13.08	157.81